IL NUOVO CIMENTO **47 C** (2024) 65
DOI 10.1393/ncc/i2024-24065-4

Colloquia: IFAE 2023

The physics of ultra-high-energy cosmic rays in the context of the Pierre Auger Observatory: Main results and future perspectives(*)

G. A. Anastasi([1])(**) for the Pierre Auger Collaboration([2])(***)(**)

([1]) *Dipartimento di Fisica e Astronomia "E. Majorana", Universitá di Catania and Sezione INFN di Catania - Catania, Italy*
([2]) *Observatorio Pierre Auger - Av. San Martín Norte 304, 5613 Malargüe, Argentina*

received 13 February 2024

Summary. — For almost 20 years, the Pierre Auger Observatory has studied ultra-high-energy cosmic rays (UHECRs) using its unique hybrid design, which employs a ground array of water-Cherenkov detectors along with 27 fluorescence telescopes to observe extensive air showers with different, complementary techniques. Some fundamental results include measurements of the energy spectrum, of the primary mass composition and of the arrival directions with unprecedented accuracy. Although no specific source has been pinpointed yet, these findings have significantly improved our understanding of UHECR and set the stage for the upgrade of the experimental setup, called AugerPrime, currently under finalization.

Introduction

Situated near the city of Malargüe in Mendoza, Argentina, the Pierre Auger Observatory [1] is the largest experimental setup dedicated to the study of ultra-high-energy cosmic rays (UHECRs) —astroparticles carrying energies larger than 10^{17} eV. Due to the exceedingly low flux, the direct observation of UHECRs is not feasible; consequently, the extensive air showers (EAS) of secondary particles produced in the interaction of primary cosmic rays with the atmospheric molecules are instead measured. The Observatory has been built incorporating both a Surface Detector (SD), comprising 1600 water-Cherenkov detectors (WCDs) organized in a 1.5 km triangular grid across approximately 3000 km^2, and 24 fluorescence telescopes positioned at the array's periphery to survey the atmosphere above the SD at elevation angles ranging from 2° to 30° (Fluorescence Detector, FD). The hybrid detection system allows to concurrently record the shower particles at ground level and the accompanying nitrogen fluorescence light emitted during the atmospheric propagation, resulting in a data-driven energy calibration and comprehensive assessment of the systematic uncertainties in both components.

(*) IFAE 2023 - "Cosmology and Astroparticles" session
(**) E-mail: gialex.anastasi@dfa.unict.it
(***) E-mail: spokespersons@auger.org
(**) Full author list: https://www.auger.org/archive/authors_2023_11.html

Throughout its almost 20 year long operational history, the Observatory has expanded its capabilities by integrating two nested dense arrays of water-Cherenkov stations with spacings of 750 m and 433 m, alongside 3 additional fluorescence telescopes with elevation coverage between 30° and 60° (High Elevation Auger Telescopes, HEAT), for measurements at energies below $\sim 10^{18}$ eV. At a later stage, the introduction of engineering arrays of underground muon detectors (Auger Muon and Infill for the Ground Array, AMIGA) and of radio antennas (Auger Engineering Radio Array, AERA) further augmented the detection capabilities of the apparatus. Finally, in 2015 the Pierre Auger Collaboration began the AugerPrime upgrade [2,3], an enhancement of the surface array designed with the primary objective of collecting new observables sensitive to the mass of UHECRs primaries.

In this contribution, some of the most striking results obtained with the data of the Pierre Auger Observatory will be presented. Moreover, the design and future perspectives of the AugerPrime upgrade will be summarized.

1. – Energy spectrum

Within the hybrid detector system of the Pierre Auger Observatory, a shower-size estimate is obtained for each event collected by the ground array, that is then calibrated against the total energy measured with the Fluorescence Detector, which delivers a nearly-calorimetric measurement of the shower energy. This approach allows the energy spectrum to be determined with minimal assumptions about hadronic interactions and about the composition of the primary particles. In particular, the energy estimate for the SD array ($E_{\rm SD}$) is determined through a calibration function $E_{\rm FD} = A\Sigma^B$, where $E_{\rm FD}$ is the FD energy, A and B the calibration parameters and Σ the SD shower-size estimator, adjusted for atmospheric attenuation using the constant intensity cut method [4]. The results for the different arrays and reconstruction procedures are shown in the left panel of fig. 1; more detailed information can be found in ref. [5] and references therein. The final systematic uncertainty in the energy scale is about 14%, mainly due to uncertainties in the FD telescopes' calibration.

The combined energy spectrum obtained with the data collected by the Pierre Auger

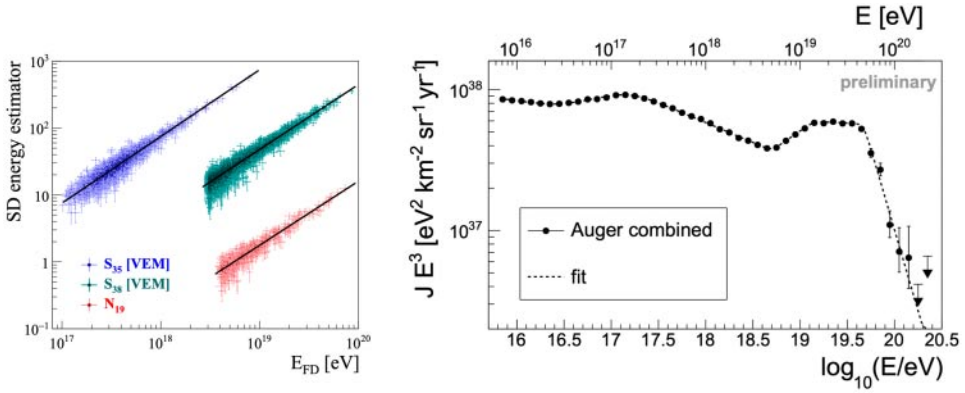

Fig. 1. – *Left*: calibration curves for the SD energy estimators as functions of the energies reconstructed by the FD. *Right*: Combined energy spectrum multiplied by E^3. The dashed line represents the fit function, sequence of six power-laws. Plots from ref. [5].

Observatory is shown in the right panel of fig. 1, together with an updated fit function characterized by six power-laws and thus five break energies. This result confirms known features, such as the cut-off at $(4.7 \pm 0.3 \pm 0.6) \times 10^{19}$ eV and the ankle at $(4.9 \pm 0.1 \pm 0.8) \times 10^{18}$ eV, but also new features, such as the break and change of spectral index identified at 1.4×10^{19} eV and referred to as *instep* [6].

2. – Mass composition

The atmospheric depth at which an EAS reaches the maximum number of particles in its development, known as $X_{\max}$, is currently considered the most reliable observable sensitive to the UHECRs mass composition. In fact, the average of the $X_{\max}$ distributions in small energy intervals is correlated with the logarithmic mass of the primary particles, while the standard deviation $\sigma(X_{\max})$ is a combination of the shower-to-shower fluctuations and of the variance of the atomic masses distribution in the primary beam [7, 8]. By observing the evolution of the first two moments of $X_{\max}$ is thus possible to infer the general trend of the mass composition in relation to the energy.

The most recent analysis is based on the data collected by the FD from 01/12/2004 to 31/12/2021; the profile reconstruction and the selection criteria are described in ref. [9] and references therein. The results confirm the presence of a transition in the evolution of the cosmic ray composition at approximately $10^{18.4}$ eV, clearly visible in the $\langle X_{\max} \rangle$ as a function of the energy, shown in fig. 2 together with a linear fit featuring a single breakpoint. Prior to this breakpoint, the average elongation rate is found to be $\sim$81 g/cm^2 per decade; post-breakpoint it is $\sim$28 g/cm^2 per decade, suggesting a transition from a lighter composition to an heavier one as the energy increases. Simultaneously, the change in the slope of the $\sigma(X_{\max})$ evolution indicates a transition from a mixed composition below $10^{18.3}$ eV to a more homogenous one at higher energies.

Observations with the fluorescence detectors offer the most precise reconstruction of $X_{\max}$ but are limited to clear, moonless nights ($\sim$14% duty-cycle). In contrast, the ground array presents a nearly 100% duty cycle but has no simple means to directly measure the shower maximum. However, certain observables related to time structure of the particle footprint on the ground, such as the signal rise time [10, 11], can be used to draw accurate conclusions regarding the average change in composition with energy. Furthermore, recent advancements in deep learning offer new tools for enhancing

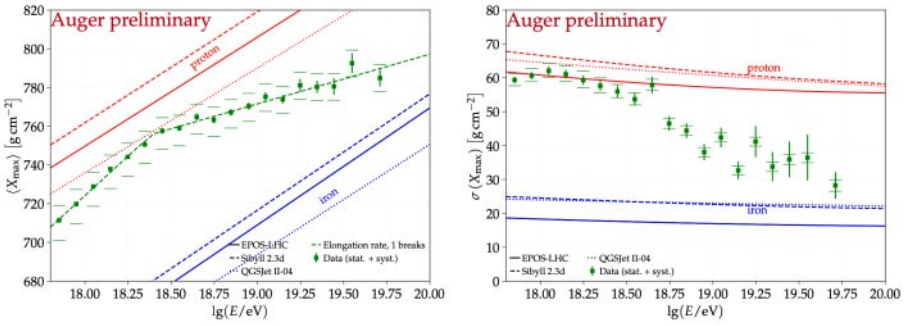

Fig. 2. – Mean $\langle X_{\max} \rangle$ (left panel) and $\sigma(X_{\max})$ (right panel) as functions of the primary energy; the predictions from different hadronic models are displayed for comparison. The fit of the elongation rate with one break a $\sim 10^{18.4}$ eV is also reported. Plots from ref. [9].

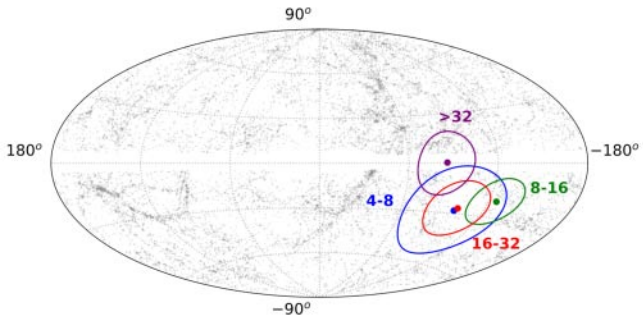

Fig. 3. – Map of the dipole direction for different energies, in Galactic coordinates. The contours are the 68% CL range, while the background black dots represent the location of the galaxies in the 2MRS catalog within 100 Mpc. Plot from ref. [15].

the reconstruction process and to obtain the depth of the shower maximum, using as inputs the time-dependent signals measured at each SD station [12, 13]. Such analysis techniques are expected to become even more powerful when applied to the data from the AugerPrime upgraded detectors, that will collect multi-hybrid events and thus allow more information to be fed both to multivariate methods and to deep neural network applications [14].

3. – Arrival direction

Understanding the origins of UHECRs inevitably involves investigating any anisotropy in their arrival directions, from which to potentially trace back to the sources of these astroparticles. The latest update in the searches for anisotropies focused on events collected by the SD from January 2004 to December 2022; the details can be found in ref. [15] and references therein.

For the analysis at large angular scales, a selection of events with primary energy above 4 EeV and zenith less than 80° has been employed, corresponding to an exposure of 123,000 km^2 sr yr and an 85% coverage of the sky. With this analysis, the significance of the dipolar modulation in right ascension [16] has reached 6.9σ for the energy range above 8×10^{18} eV, increasing with respect to previous results. The direction of this dipole is 113° away from the Galactic Center (see fig. 3), indicating that the cosmic rays above this energy threshold likely have an extragalactic origin.

Other notable findings [17] include: i) the observation of an overdensity in the Centaurus region with a post-trial p-value of 3.0×10^{-5}, equivalent to a 4σ significance; ii) a correlation with the catalog of starburst galaxies, determined via a likelihood test, showing a post-trial p-value of 6.6×10^{-5} or 3.8σ significance.

4. – The AugerPrime upgrade

To further advance our understanding of UHECR, the Pierre Auger Observatory is currently finalizing an upgrade of the SD, named AugerPrime [2, 3]. The goal is to provide an accurate determination of the mass composition at the highest end of the energy spectrum, addressing the limitation of the FD event statistics above $\sim 10^{19.5}$ eV (mainly due to its reduced duty cycle).

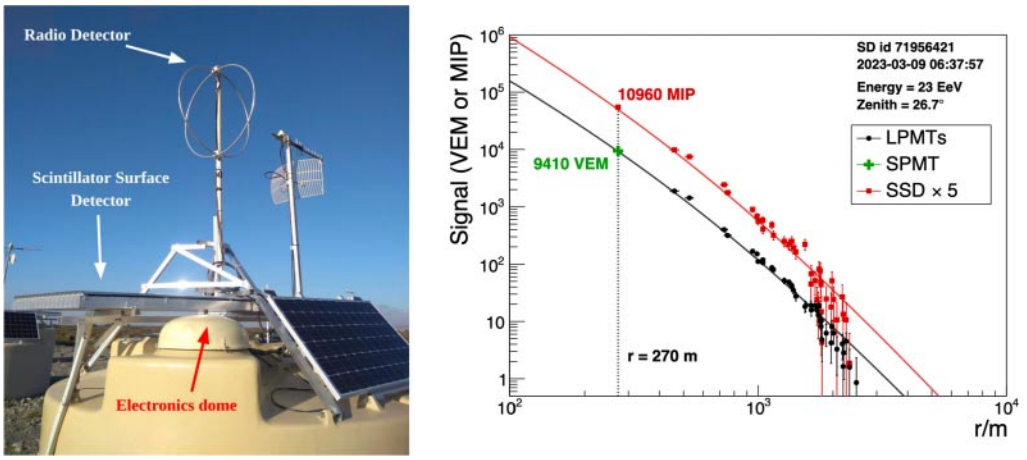

Fig. 4. – *Left*: an upgraded station; the SSD and the radio antenna positioned on top of the WCD are indicated. Photo from ref. [24]. *Right*: shower signals collected by the AugerPrime detectors (with SSD signals multiplied by a factor 5 for clarity) for a 23 EeV event arriving at a zenith angle of 26.7°; the continuous lines indicate the reconstructed Lateral Distribution Functions. In the station nearest to the shower core the standard 9-inch PMTs in the WCD are saturated, thus the SPMT signal is used. Plot from ref. [20].

The upgrade includes the addition, on top of each existing WCD (see left panel of fig. 4), of a $\sim$2 m^2 scintillator surface detector (SSD) [18] and of a radio detector (RD) [19] consisting of a dual-polarized antenna designed for a frequency range of 30-80 MHz. To minimize signal saturation, a small 1-inch photomultiplier (SPMT) is installed in each WCD [20]. Additionally, underground muon detectors (UMDs) [21], which are plastic scintillators buried 2.3 m underground, are placed in the nested 750 m and 433 m arrays to directly measure the muon component of air showers. The surface detector electronics is updated with the deployment of the Upgraded Unified Board (UUB) [22], featuring a new analog-to-digital converter with 120 MHz sampling. The UUB ensures backward compatibility with previous measurements and accommodates channels for the new detectors. The DAQ software has also been updated [23].

The upgraded station is designed to disentangle the muonic and electromagnetic (e^+, e^-, γ) components of EASs on an event-by-event basis, to determine not only the $X_{\max}$ but also the number of muons (another indicator of the primary mass) especially in the region of the flux suppression. To this aim, the different responses of SSDs and WCDs to the shower particles will be exploited in vertical (zenith $< 60°$) events, while the RD and WCD signals will be compared in more inclined events([1]). The UMD measurements will provide constraints for these studies, although in a lower energy range.

By July 2023, the installation of SSDs, SPMTs and UUBs across the entire array was completed [24], while the deployment of UMDs and radio antennas is scheduled to be completed around mid-2024. An examplary high-energy event, measured with the upgraded SD array, is shown in the right panel of fig. 4.

([1]) In inclined showers, only muons reach the ground and release a signal in the WCDs. The e.m. component is absorbed in atmosphere, anyway having produced detectable radio emission.

Conclusions

The study of UHECRs with energies above 10^{17} eV remains a critical area of research even more than a century after Victor Hess' initial discovery. While a comprehensive theoretical framework encompassing the origin, acceleration mechanisms, and exact composition of UHECRs is still under development, significant advancements have been made through the analysis of data from the Pierre Auger Observatory (see for example ref. [25]). While some fundamental findings have been described in this contribution, other noticeable results have been overlooked for the sake of brevity, such as: the evidence of a 20-30% muon deficit in the current models for hadronic interactions [26, 27], the searches for UHE photons and neutrinos [28,29], the studies of energetic atmospheric phenomena [30,31] and much more.

In the next decade, the increased sensitivity to the mass composition of UHECR with extreme energies (namely above above $\sim 4 \times 10^{19}$ eV) granted by the AugerPrime upgrade will help to unravel the remaining mysteries in the cosmic rays field and will deliver fundamental insights to be used by the next generation of experiments.

REFERENCES

[1] Aab A. *et al.*, *Nucl. Instrum. Methods A*, **798** (2015) 172.
[2] Aab A. *et al.*, arXiv:1604.03637 [astro-ph.IM] (2016).
[3] Castellina A., *EPJ Web of Conferences*, **210** (2019) 06002.
[4] Aab A. *et al.*, *JINST*, **15** (2020) P10021.
[5] Novotný V., *PoS*, **ICRC2021** (2021) 324.
[6] Aab A.*et al.*, *Phys. Rev. Lett.*, **125** (2020) 121106.
[7] Aab A. *et al.*, *Phys. Rev. D*, **90** (2014) 122005.
[8] Aab A. *et al.*, *Phys. Rev. D*, **90** (2014) 122006.
[9] Fitoussi T., *PoS*, **ICRC2023** (2023) 319.
[10] Aab A. *et al.*, *Phys. Rev. D*, **96** (2017) 122003.
[11] Todero Peixoto C. J., *PoS*, **ICRC2019** (2019) 440.
[12] Aab A. *et al.*, *JINST*, **16** (2021) P07019.
[13] Glombitza J., *PoS*, **ICRC2023** (2023) 278.
[14] Langner N., *PoS*, **ICRC2023** (2023) 371.
[15] Golup G., *PoS*, **ICRC2023** (2023) 252.
[16] Aab A. *et al.*, *Science*, **357** (2017) 1266.
[17] Aab A. *et al.*, *ApJ*, **935** (2022) 170.
[18] Cataldi G., *PoS*, **ICRC2021** (2021) 251.
[19] Pawlowsky J., *PoS*, **ICRC2023** (2023) 344.
[20] Anastasi G. A., *PoS*, **ICRC2023** (2023) 343.
[21] de Jessús J., *PoS*, **ICRC2023** (2023) 267.
[22] Abdul Halim A. *et al.*, *JINST*, **18** (2023) P10016.
[23] Sato R., *PoS*, **ICRC2023** (2023) 373.
[24] Convenga F., *PoS*, **ICRC2023** (2023) 392.
[25] Abdul Halim A. *et al.*, *JCAP*, **05** (2023) 024.
[26] Aab A. *et al.*, *Eur. Phys. J. C*, **80** (2020) 751.
[27] Aab A. *et al.*, *Phys. Rev. Lett.*, **126** (2021) 152002.
[28] Abreu P. *et al.*, *Universe*, **8** (2022) 579.
[29] Niechcio M.ł, *PoS(ICRC2023)*, **2023** (1488) .
[30] Aab A. *et al.*, *Earth Space Sci.*, **7** (2020) e2019EA000582.
[31] Colalillo R., *PoS*, **ICRC2023** (2023) 439.